

SHEAR CONTROLLED SWIRL JETS BY HELICAL PERTURBATION WAVE

Wonjoong Lee*, Ieeki Ahn*
*Korea Aerospace Research Institute

Keywords: *swirl jet, helical mode, shear layers, passive control, vortex core*

Abstract

To explore the possibility of using artificial means for the control of shear layers in swirl jet, a novel control device for swirling jets is designed. The device consists of a tube with internal lobes (i.e., convex surfaces) of small height to induce disturbance. The number of convexities can be varied to induce helical modes in azimuthal direction. The velocity and turbulence intensity of the swirling jet, with and without the lobes, are numerically simulated at the various distances from the nozzle exit. The results are compared with the baseline at various helical modes. It is observed that the artificial excitation approach is effective in the control of the vortical structure in swirling jets.

Nomenclature

D: nozzle exit diameter
Re: Reynolds number
m: helical mode
v: velocity magnitude
S: swirl number

1. Introduction

Jet flow control is one of the major interests in the field of flow control society. Flow control is generally divided into two parts, active or passive, according to the putting energy into the flow or not. In case of the active control which is relatively more investigated by many researchers, the fundamental approach begins with the generating artificial flow turbulence or the supplying momentum and energy into the boundary layer. By enhancing

the turbulence mixing rate or increasing the energy entrainment from the outside of boundary layer into the inside, the active control changes the flow characteristics, especially retarding or preventing flow separation.

Low amplitude acoustic excitation of swirling jets using plane waves has been tried in the past on the swirling jets at low swirl number^[1,2]. The non-dimensional swirl number is defined as the angular momentum flux divided by axial momentum flux, times the nozzle exit radius. In these experiments, the jet's swirl number was 0.35 and the excitation sound pressure level was 126dB. In spite of the maximum growth of the instability waves at excitation Strouhal number of 0.4, no change in the mixing characteristics of the swirling jet was observed in these experiments. Mixing enhancement by plane wave excitation was only achieved when high amplitude, electro-pneumatic excitation devices (Ling drivers, capable of generating 170dB SPL in the near field), were used to excite a swirling jet at low swirl numbers of $S=0.12$ ^[3]. Generation of pure and controllable helical waves to excite these natural, fast-growing instability waves has always been a challenge^[4]. Motivated by the above arguments, the following research activities are carried out:

- A unique system is designed to incorporate a novel, robust passive control device that is capable of generating helical waves, mechanically rather than acoustically which has traditionally been done. It facilitates future design for practical applications.
- The above system is used to excite the natural instabilities (Kelvin-Helmholtz)

of a swirling jet at different modes ($m=0$, $m=1$, $m=2$, $m=3$, $m=4$, and $m=5$, where m is the azimuthal wave number).

- The effects of growth of natural helical instability waves of different modes on vortex core and shear layer of a swirling jet are numerically demonstrated.

2. Numerical Analysis

2.1 Numerical Set-up

A commercial code, FLUENT V6.1 which is based on Navier-Stokes equation is utilized for this analysis. FLUENT can analyze the viscous flow, and it's preprocessor, GAMBIT has 'Journaling Function' for auto grid generation. This function is useful to mesh the similar type models repeatedly^[5]. SST $k-\omega$ is selected as the turbulence model, which is a variant of the standard $k-\omega$. This model combines the original Wilcox model (1988) for use near walls and standard $k-\epsilon$ model away from wall using a blending function. It is also known as appropriate for rotating flow. The Reynolds number and mass flow rate of the swirl jet are 6.9×10^4 and 0.08 kg/sec respectively.

2.2 Computational Layout

The computational domain is shown in figure 1 through 3. It consists of swirl generator, subsonic nozzle, excitation device, and free jet expansion region. The swirl generator (Fig. 2) with 30 degree incidence angle can produce swirl jet flow. The helical disturbances are induced on the swirling jet by internal contoured lobes located on the inside surface of the cylinder (Fig. 3). The upstream and downstream ends of the lobes are contoured flush with the inner-surface of the circular nozzle exit to provide a smooth transition. Therefore it prevents the flow separation at these locations. Identical cylinders with zero (no lobe; baseline configuration), one, two, three, four, and five lobes are used in this analysis, simulating total

five helical-instability modes; i.e., $m=1, 2, 3, 4$, and 5 (Fig. 4).

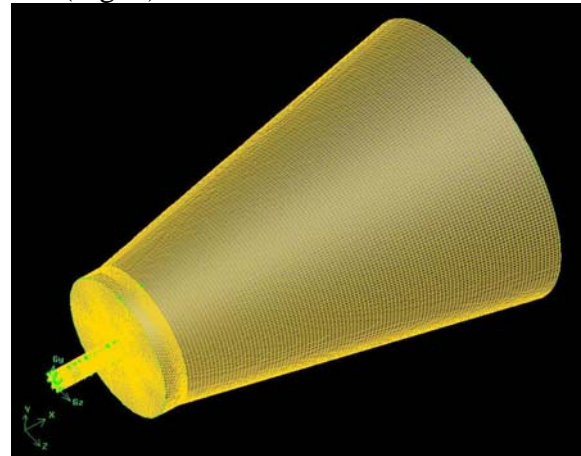


Fig. 1. Computational domain and grid generation

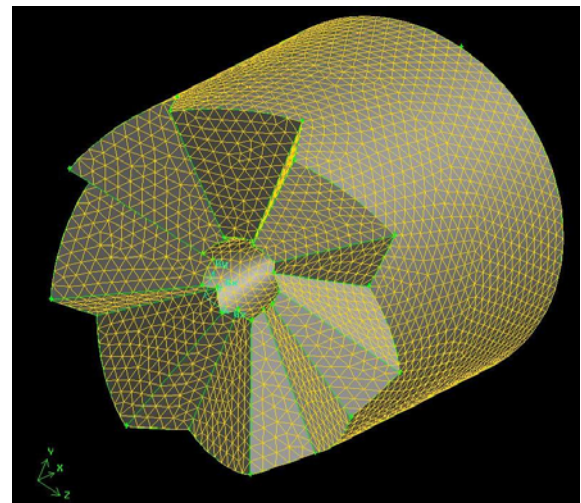


Fig. 2. Grid for the swirl generator

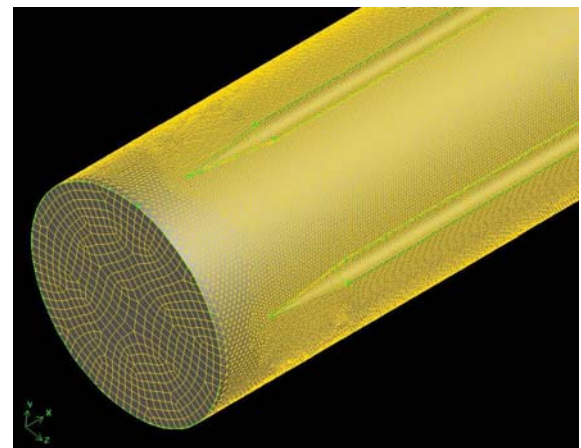


Fig. 3. Grid for the excitation device

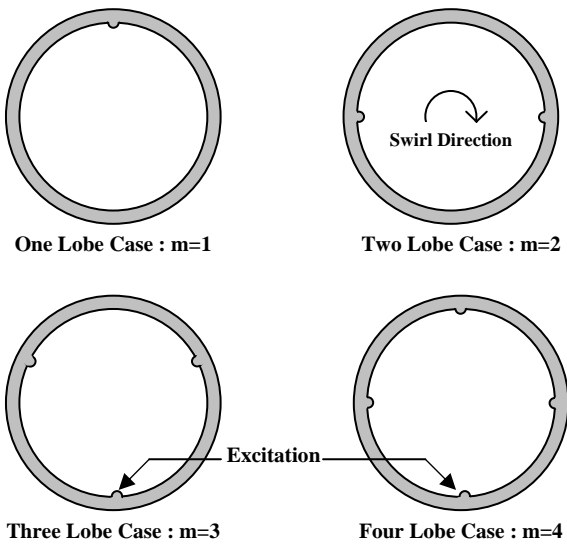


Fig. 4. Layout of excitation disturbances on the inner tube surface

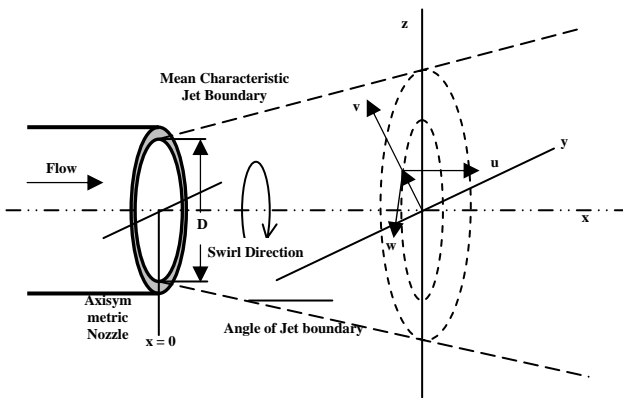


Fig. 5. Definition sketch for an axisymmetric swirl jet

3. Results

The effects of excitation on the growth of the natural helical instability waves are investigated by the velocity magnitude and fluctuating quantities of the excited swirling jet. A definition sketch is shown in figure 5. Comparison of the velocity and turbulence intensity profiles between jets at various excitation modes provides a unique indication of the jet characteristics. Plotting is executed in two ways (i.e., one dimensional line plots and two dimensional contour plots). Line plots show the detail velocity (or turbulence intensity) profile of vortex core which is presented along the centerline or in radial distribution. Contour

plots show the same velocity distribution by using closed lines in an equivalent level.

3.1 Centerline Distribution

The centerline distribution plots of the velocity magnitude and turbulence intensity are arranged together in figures 6 through 7 for the purpose of easy comparison of the axial velocity distributions.

3.1.1 Velocity Magnitude

Figure 6 shows the vortex core velocity distribution along the centerline from the jet exit to 20 nozzle diameters downstream from the nozzle exit (i.e., $x/D=0\sim 20$). Even though the lobes are small and attached to the inner surface of the cylinder, there are significant effects on the velocity profile at the center part of vortex core. As shown in figure 6, all the swirl jets have lower velocities (7~8m/s) at the nozzle exit compared to the round jet case (13.7m/s). Furthermore velocity distributions are characterized depend on the various helical modes ($m=1\sim 5$). Right after departing the nozzle exit the swirl core velocity rapidly increases approximately 60% compared to the nozzle exit one. The augmented velocities maintain up to the axial location of $x/D=7.5$, and especially in case of $m=4$, the effect dominates throughout the displayed entire downstream region.

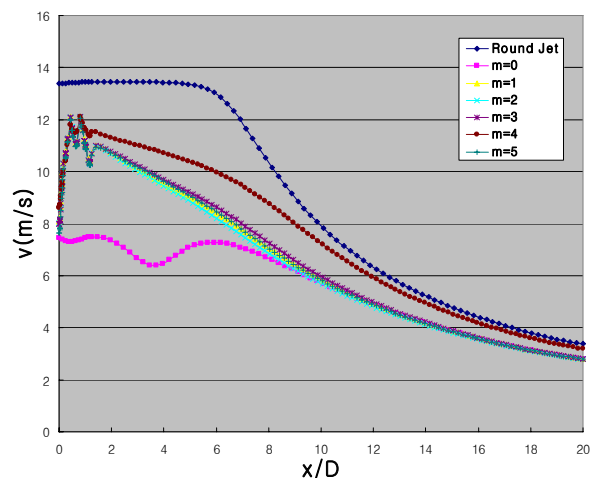


Fig. 6. Centerline distributions of velocity magnitude at various helical modes

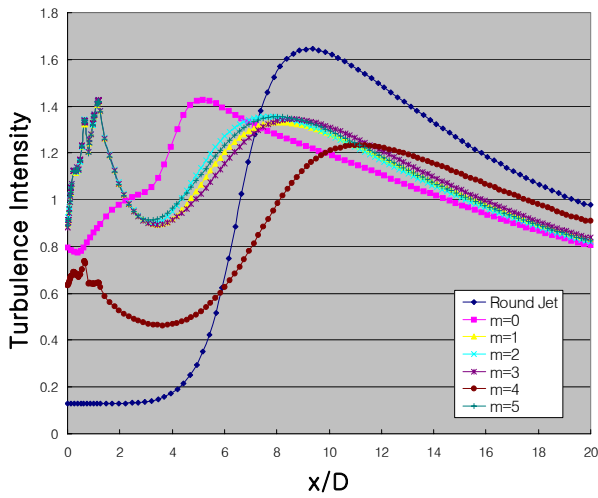


Fig. 7. Centerline distributions of velocity magnitude at various helical modes

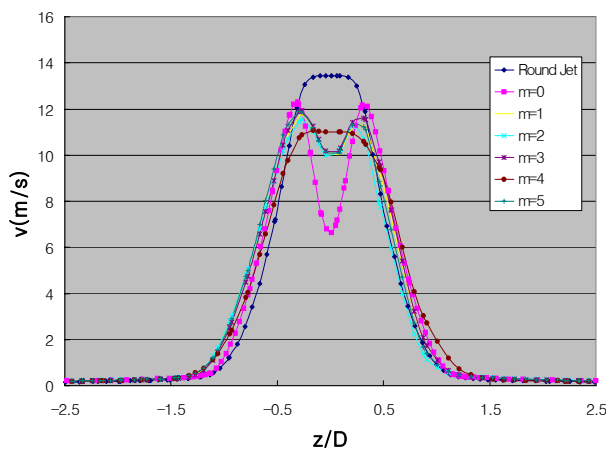


Fig. 8. Radial distributions of velocity magnitude at various helical modes

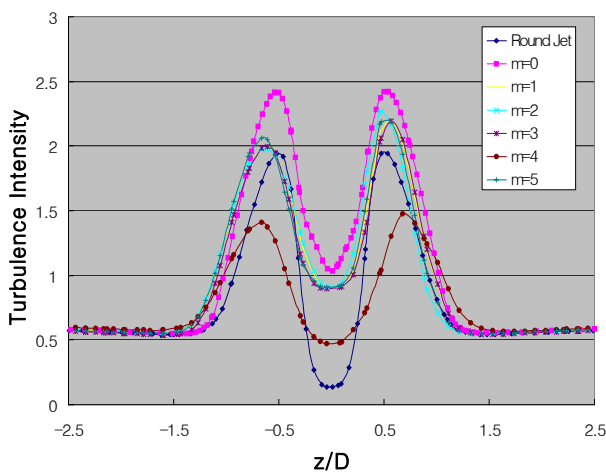


Fig. 9. Radial distributions of turbulence intensity at various helical modes

3.1.2 Turbulence Intensity

Figure 7 shows the turbulence intensity distribution of vortex core along the centerline between $x/D=0$ and 20. Expected from the results of velocity magnitude, there is similar trend in turbulence intensity distribution. As shown in figure 7, compared to the round jet case, all the swirl jets have higher intensity values at $x/D=0$ through 7.5. Also for the most of helical disturbances ($m=1, 2, 3,$ and 5) except for $m=4$ case, the turbulence intensity is increased at the near exit region compared to the baseline.

3.2 Radial Distribution

Fig. 8 and 9 show the comparison of radial profiles (variations in z/D traverse) of velocity magnitude and turbulence intensity respectively at $x/D=3$ & $y/D=0$ for various helical modes.

3.2.1 Velocity Magnitude

As expected in section 3.1, figures 8 & 9 show noticeable effects on the velocity profile of the vortex core as well as the shear layer. It is revealed that helicities ($m=1$ to $m=5$) reduce the depth of the double hump profile which is formed due to the wake effect of the central cone of the vortex generator. The maximum velocity of $m=4$ case is down by 8.8% compared to $m=0$ case, and the center velocity is up by 74.1%. Especially in case of $m=4$, the wake effect by the central cone is diminished, and it forms the flat shape similar to the round jet. It reveals that there is a specific helical perturbation mode according to the swirl jet flow for the purpose of controlling vortex fading.

3.2.2 Turbulence Intensity

All the helical perturbation cases reduce the turbulence intensity in comparison with baseline ($m=0$). In case of $m=4$ which has no wake effect in velocity profile, the turbulence intensity variation is minimized, and its peak value is down by 40.8% compared to the baseline's. The turbulence intensity profile also spreads out widely in radial direction ($z/D=-0.7\sim+0.7$) simultaneously.

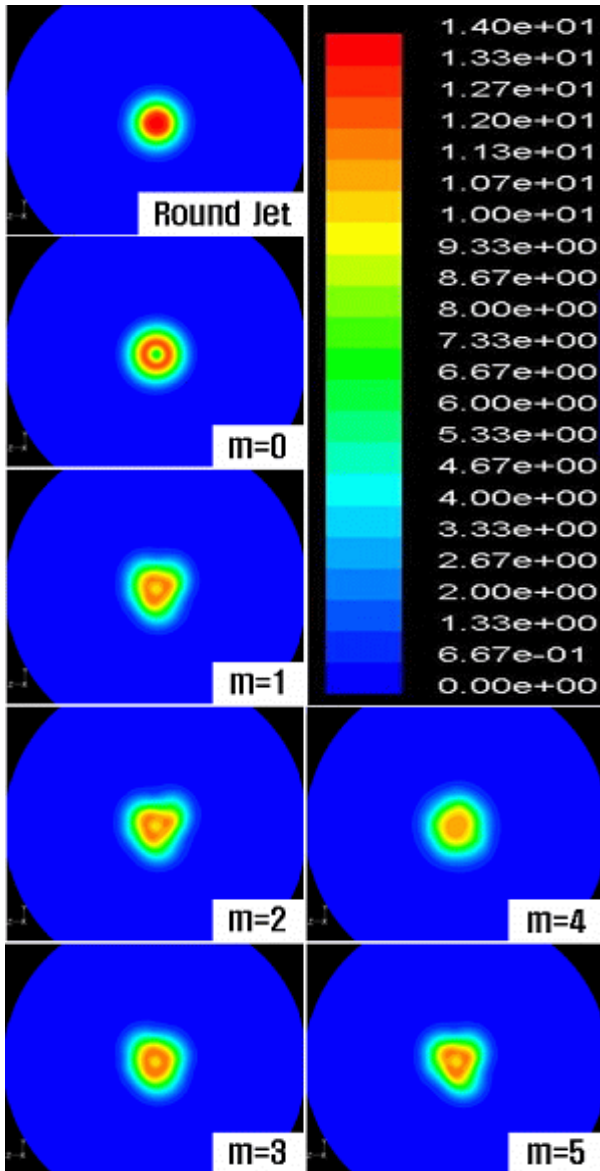


Fig. 10. Contours of velocity at $x/D=3$ for various helical modes

3.3 Velocity Contour

Detailed velocity magnitude contours are made in the jets, on a plane perpendicular to the centerline at 3 nozzle diameters downstream from the nozzle exit ($x/D=3$). The effects of excitation on the velocity distribution of this swirling jet, excited at various helical modes, are plotted selectively in figure 10. The case of $m=0$ (with no lobes) is also used as the baseline. In addition, in figures 12 through 15, the contours of velocity magnitude at various axial

locations for the selective cases ($m=4$ & 5) are presented.

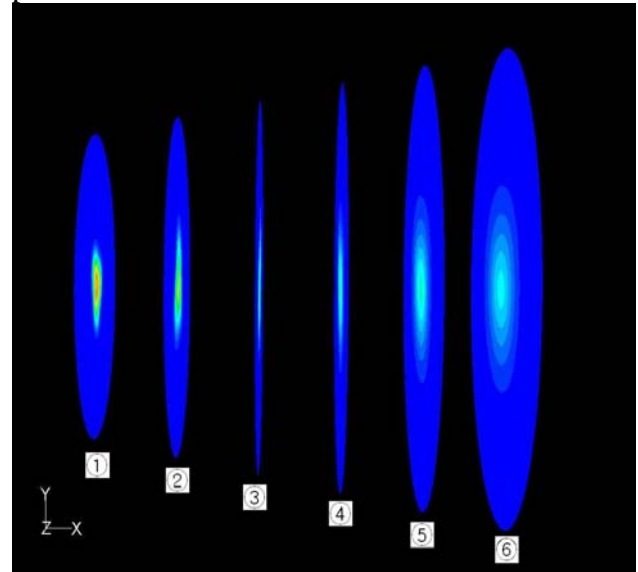


Fig. 11. Axial locations of contour plots from the nozzle exit

- ① $x/D=03.75$ ② $x/D=06.25$ ③ $x/D=08.75$
- ④ $x/D=11.25$ ⑤ $x/D=13.75$ ⑥ $x/D=16.25$

3.3.1 Velocity Contour at $x/D=3$

Figure 10 shows the contours of velocity at $x/D=3$ for various helical perturbation modes. The outer contour lines of helical disturbance cases have more irregular pattern than the baseline ones. In case of $m=0$, the contour lines have circular shape, but all the helicity applied cases ($m=1\sim5$) have the distorted contour lines. It is also found that $m=4$ case which shows most noticeable effect in vortex core analysis has least influence in the jet boundary profile. For the purpose of boundary shear control, it reveals that $m=2$ (or $m=5$) are more effective than any other cases.

3.3.2 Velocity Contour Comparison ($m=4$ & 5)

To explore the velocity variation in axial direction, the velocity contour plots are displayed at various stations (Fig. 11). Among five helicities ($m=1\sim5$), two distinctive cases ($m=4$ & 5) are compared each other. Figure 12 shows that the near exit region (a, b) has small influence by helical disturbance, but there is no remarkable effect at d, e, and f. As can be seen in figure 12 (d), (e), (f), the contour lines return to the circular shape similar to the baseline as flow travels along the center line.

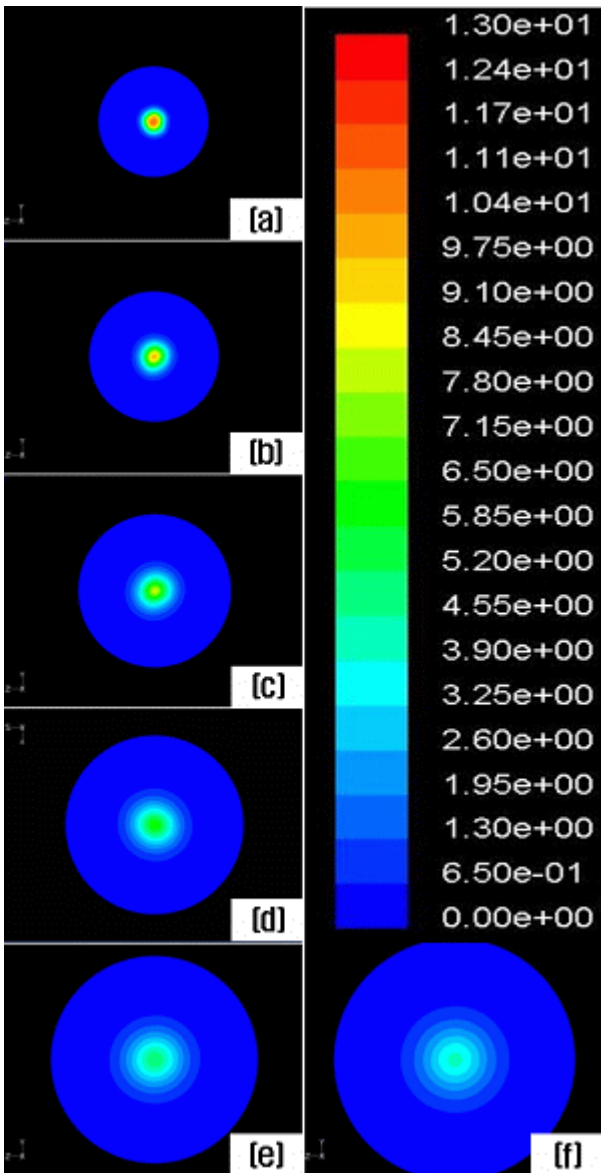


Fig. 12. Contours of velocity magnitude at various axial locations (m=4)

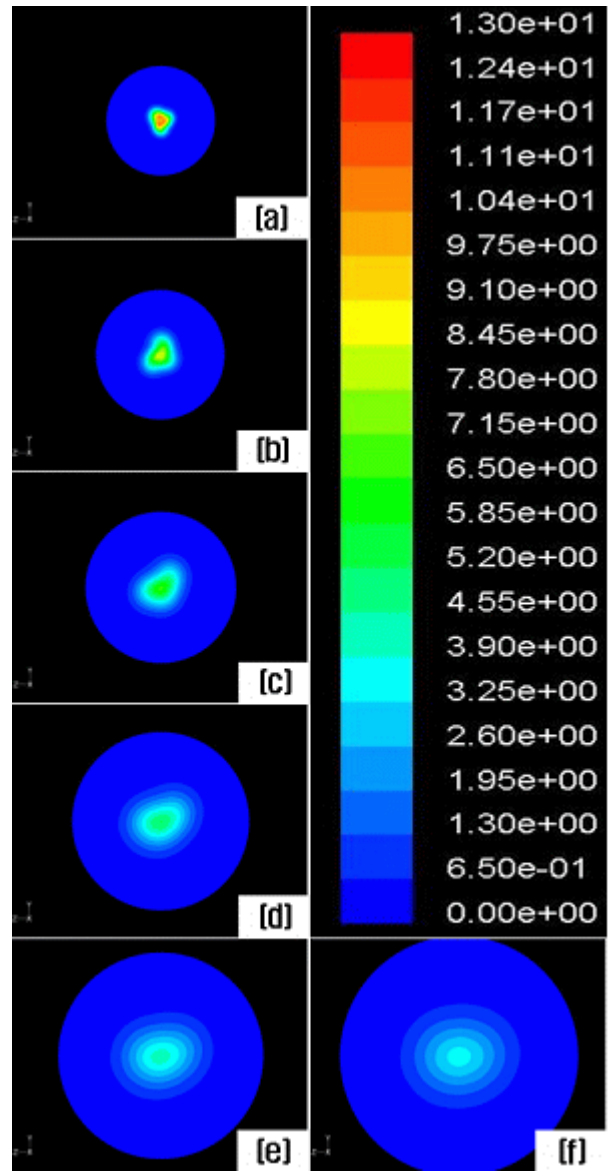


Fig. 14. Contours of velocity magnitude at various axial locations (m=5)

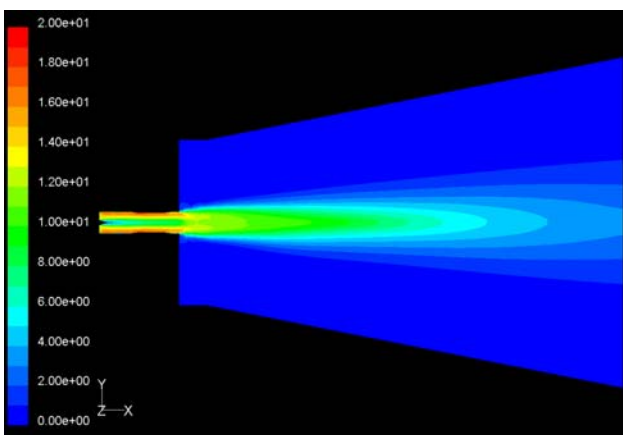


Fig. 13. Contour of velocity magnitude at z-normal plane (m=4)

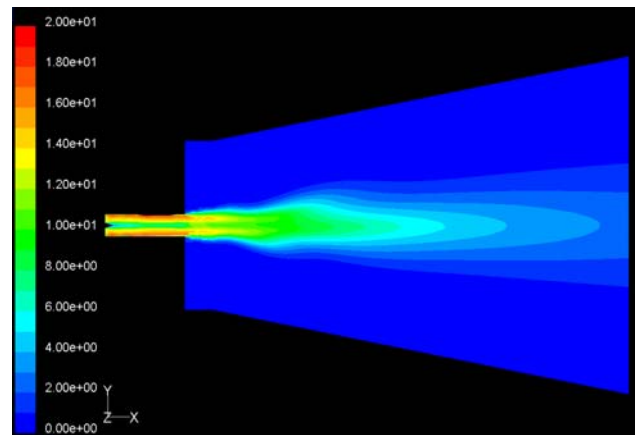


Fig. 15. Contour of velocity magnitude z-normal plane (m=5)

The case of $m=5$ (Fig. 14 & 15) presents a contrast to baseline (or even $m=4$), and it shows the most noticeable effects by helical disturbance. Throughout the entire downstream region, it shows fairly distorted contour lines different from the circular ones. As marching down to the axial direction, the irregular contour lines are changed into elliptic shape, and these are distinguished from the $m=4$ cases.

4. Conclusion

A passive control device for helical-wave excitation of swirling jets was designed and examined. To reveal the effect of the device, numerical modeling and simulation of major flow properties were carried out.

In this study, the fact^[6-8] that the initial disturbance on axisymmetric jet exit affects the development of the large-scale vortical structure which is in near exit area was also confirmed for swirling jet. It was shown that the response of the swirling jet to helical-mode excitation not only affects the shear layer areas, but also strongly affects the vortex core. It is also observed that there is a preferred mode for swirl control.

This study brought the possibility of selective control depends on the control purposes (e.g. vortex core or jet boundary).

References

- [1] Farokhi, S., and Taghavi, R., and Rice, E.J., 1988, Controlled Excitation of a Cold Turbulent "Swirling Free Jet, *Transactions of ASME, Journal of Vibration, Acoustics, Stress, and Reliability in Design*, Vol. 110, No.2.
- [2] Farokhi, S., and Taghavi, R., 1988, Turbulent Swirling Jets with Excitation, *NASA CR-180895*.
- [3] Taghavi, R., Rice, E.J., and Farokhi, S., 1989, Large Amplitude Acoustic Excitation of Swirling Turbulent Jets, *AIAA-89-0970*.
- [4] Taghavi, R. and Han, S. Computational Study of Supersonic Jets from Swirl Inducing Nozzles, *AIAA-2001-0673* at the 39th *AIAA Aerospace Sciences Meeting*, Reno, Nevada, Jan. 8-22, 2001.
- [5] *FLUENT Inc., FLUENT 6 User's Guide*, 2001.
- [6] Ho, C. M. and Huerre, P., 1984, Perturbed Free Shear Layers, *Ann. Rev. Fluid Mech.*, Vol. 16. pp. 365-424.
- [7] Thomas, F. O., 1991, Structures of Mixing Layers and Jets, *Appl. Mech. Rev.*, Vol. 44, No. 3, pp. 119-153.
- [8] Mankbdi, R. R., 1992, Dynamics and Control of Coherent Structure in Turbulent Jets, *Appl. Mech. Rev.*, Vol. 45, No. 6, pp. 219-247.